J Solid State Electrochem (2007) 11:1109–1117
DOI 10.1007/s10008-006-0247-3

ORIGINAL PAPER

Layer-by-layer deposition of open-pore mesoporous TiO_2-Nafion® film electrodes

Elizabeth V. Milsom · Jan Novak · Stephen J. Green · Xiaohang Zhang · Susan J. Stott · Roger J. Mortimer · Karen Edler · Frank Marken

Received: 15 October 2006 / Revised: 13 November 2006 / Accepted: 17 November 2006 / Published online: 3 January 2007

Abstract The formation of variable thickness TiO_2 nanoparticle-Nafion® composite films with open pores is demonstrated via a layer-by-layer deposition process. Films of about 6 nm diameter TiO_2 nanoparticles grow in the presence of Nafion® by "clustering" of nanoparticles into bigger aggregates, and the resulting hierarchical structure thickens with about 25 nm per deposition cycle. Film growth is characterized by electron microscopy, atomic force microscopy, and quartz crystal microbalance techniques. Simultaneous small-angle X-ray scattering and wide-angle X-ray scattering measurements for films before and after calcination demonstrate the effect of Nafion® binder causing aggregation. Electrochemical methods are employed to characterize the electrical conductivity and diffusivity of charge through the TiO_2-Nafion® composite films. Characteristic electrochemical responses are observed for cationic redox systems (diheptylviologen$^{2+/+}$, $Ru(NH_3)_6^{3+/2+}$, and ferrocenylmethyl-trimethylammonium$^{2+/+}$) immobilized into the TiO_2-Nafion® nanocomposite material. Charge conduction is dependent on the type of redox system and is proposed to occur either via direct conduction through the TiO_2 backbone (at sufficiently negative potentials) or via redox-center-based diffusion/electron hopping (at more positive potentials).

E. V. Milsom · J. Novak · S. J. Green · X. Zhang · K. Edler · F. Marken (✉)
Department of Chemistry, University of Bath,
Bath BA2 7AY, UK
e-mail: f.marken@bath.ac.uk

S. J. Stott · R. J. Mortimer
Department of Chemistry, Loughborough University,
Loughborough LE11 3TU, UK

Keywords Voltammetry · TiO_2 · Nafion® · Electron hopping · Sensor · Mesoporous film · Photoelectrochemistry · Electrode

Introduction

Mesoporous oxides are commonly used in sensors [1], photovoltaic devices [2], and in catalyst support systems [3]. In particular, titanium oxide has been found to have many applications [4] and is commonly applied in the form of mesoporous calcined films [5]. New alternative strategies for the deposition of ordered TiO_2 films include nanotube growth [6] and sol-gel dip-coating [7], but the more commonly employed direct deposition of nanoparticulate material is usually sufficient for most thin film applications. Porous membranes of TiO_2 have been formed by doctor-blading [8], printing [9], and by layer-by-layer deposition [10] of an alternating sequence of a negatively charged binder and the positively charged nanoparticulate TiO_2.

The layer-by-layer deposition of mesoporous oxides is versatile, reproducible, and ideal for the formation of thin coatings on electrode surfaces [11]. The methodology, initially developed by Decher [12], allows molecular binders [13], ionomeric binders [14], and other types of nanoparticles [15] to be incorporated into the growing film. In this study, the effect of employing Nafion® ionomer as a binder for TiO_2 nanoparticles is explored (see Fig. 1).

Although layer-by-layer deposition is possible with small molecular binders, higher molecular weight ionomers such as Nafion® are known to produce a more stable film [16]. The thickness of a single layer of a film depends on factors such as the weight, size and concentration of the polyelectrolyte binder, and of the charged species. Intermolecular forces, hydrophobic forces [17], and hydrogen

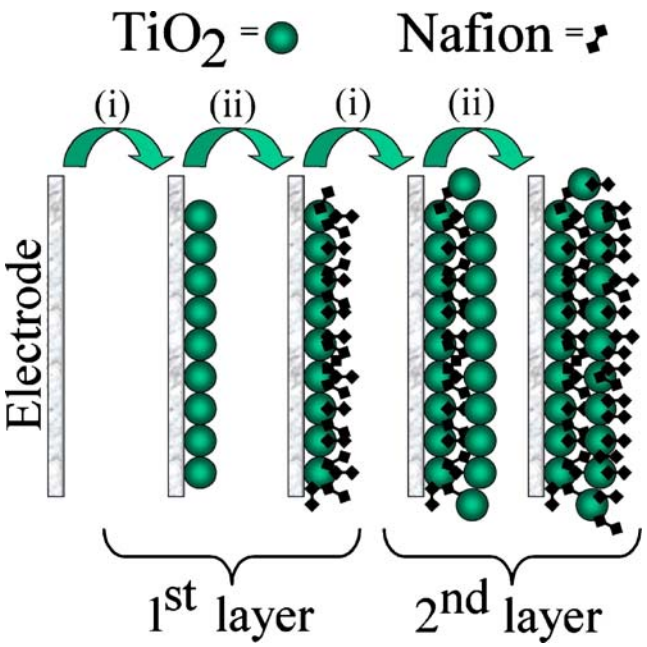

Fig. 1 Schematic representation of the layer-by-layer deposition process involving, (*i*) immersion of the ITO substrate into the positively charged nanoparticle solution, followed by rinsing steps, and (*ii*) immersion into Nafion® anionomer solution followed by rinsing steps

bonding [18] have all been reported to have an effect on the structure of the deposited films.

Composites of Nafion® (a chemically inert fluorocarbon with sulfonic acid groups [19]) and TiO_2 have been proposed for example for applications in proton-conducting membranes [20], in fuel cells [21], in photoelectrochemical devices [22], for photochemical degradation membranes [23], employed for dopamine sensing [24], and for nitric oxide sensing [25], and they have been produced with Langmuir–Schäfer techniques [26]. The combination of the chemically robust Nafion® binder with the mesoporous structure formed by the TiO_2 nanoparticle backbone results in a very interesting and widely applicable thin film structure.

In this study, TiO_2 nanocomposite films are constructed from a Nafion® ionomer binder and about 6 nm diameter TiO_2 nanoparticles. A simple dip coating approach allows films of variable thickness to be formed and investigated. Perhaps surprisingly, an open-pore structure is formed consisting primarily of the TiO_2 backbone and a thin film of Nafion® at the surface. Voltammetric measurements in aqueous solution suggest that the charge transport at potentials negative of about −0.7 V vs saturated calomel electrode (SCE) is dominated by electron conduction through the TiO_2 backbone, whereas at more positive potentials, diffusion of redox species and inter-molecular electron hopping are dominating. The rate for charge transport in the positive potential range is very similar to that measured for conventional bulk Nafion® films.

Experimental

Chemical reagents

Nafion® perfluorinated ion-exchange resin (5 wt%, in a mixture of lower aliphatic alcohols and H_2O), $NaClO_4$, KCl, 1,1′-diheptyl-4,4′-bipyridinium dibromide or diheptylviologen, $Ru(NH_3)_6Cl_3$, ferrocenylmethyl-trimethylammonium iodide (all Aldrich) were obtained commercially and used without further purification. TiO_2 sol (about 6 nm diameter, anatase, 30–35% in aqueous HNO_3, pH 0.5, TKS-202) was obtained from Tayca, Japan. Solutions were prepared using filtered and deionized water with a resistivity of not less than 18 MΩ cm.

Instrumentation

Voltammetric experiments were performed with a Micro-Autolab III system (Eco Chemie, The Netherlands) in a standard three-terminal electrochemical cell with a SCE (Radiometer, Copenhagen) placed about 0.5 cm from the working electrode and a 2×2 cm platinum gauze counter electrode. The working electrodes were made from tin-doped indium oxide (ITO) coated glass (10×60 mm, 15 Ω per square, Image Optics, Basildon, UK). The ITO electrode was rinsed with ethanol and water, heat-treated in a furnace (Elite Thermal Systems) for 1 h at 500 °C and re-equilibrated to ambient conditions before use. Before the voltammetric experiments solutions were de-aerated with argon (BOC). All experiments were conducted at a temperature of 22±2 °C.

Quartz crystal microbalance experiments were conducted with ITO-coated quartz crystals (Part no. QA-A-9M-ITOM, Advanced Measurement Technology, Wokingham, Berks). A quartz crystal oscillator circuit (Oxford Electrodes) connected to a frequency counter (Fluke, PM6680B) allowed the resonance frequency of the quartz crystal sensor to be monitored. The 9.1 MHz AT-cut quartz crystal microbalance system was calculated [27] to have a sensitivity factor of $\frac{\Delta m}{\Delta f} = -1.05\ \mathrm{ng\,Hz^{-1}}$ in air based on the expression $\frac{\Delta m}{\Delta f} = -\frac{A\times\sqrt{\mu_Q\rho_Q}}{2f_0^2}$ with the area A=0.2 cm^2, the resonance frequency f_0=9.1×10^6 Hz, the density of quartz ρ_Q=2.648 g cm^{-3}, and the shear modulus of quartz $\mu_Q = 2.947 \times 10^{11}\ \mathrm{g\,cm^{-1}s^2}$.

Field emission gun scanning electron microscopy (FEG-SEM) images were obtained on a Leo 1530VP field emission gun SEM system. A SAXS/WAXS (simultaneous small-angle X-ray scattering and wide-angle X-ray scattering) pattern of the TiO_2-Nafion® films was obtained on a

SAXSess system using a PW3830 X-ray generator, and the X-ray image plates were observed using a Perkin Elmer cyclone storage phosphor system. A TiO_2-Nafion® film (50 deposition cycles on a microscopy cover plate) was produced and the patterns recorded in transmission mode with Cu Kα radiation (λ = 1.5406 Å) at 40 kV and 50 mA with an exposure time of 20 min. A background pattern from a clean cover plate was subtracted and the data corrected for slit smearing before fitting.

Layer-by-layer deposition of TiO_2-Nafion® films

The deposition procedure consisted of a sequence of liquid immersion steps with (1) a TiO_2 sol (6 nm diameter, 3 wt% in nitric acid, pH about 2) for 60 s followed by rinsing with distilled water and methanol, (2) dipping into Nafion® anionomer solution (about 3 wt% in methanol) for ~10 s followed by rinsing with methanol and distilled water. This completed a single layer deposition for the simple TiO_2-Nafion® film, and the cycle was repeated to add more layers.

Results and discussion

Layer-by-layer formation of TiO_2-Nafion® nanocomposite film electrodes

Nafion® is an anionic polymer which is widely used as an ion-exchange membrane material [28] or as a protective semipermeable coating [29]. Solutions of Nafion® in aliphatic alcohols are employed for the formation of thin films, and in this study, a dilute solution of Nafion® in methanol (0.3 wt%) is employed to act as a binder to grow thin films of a novel open-pore TiO_2-Nafion® composite membrane. An aqueous TiO_2 sol provides the source of positively charged TiO_2 nanoparticles of nominal 6 nm diameter, which are deposited with the Nafion® binder in a layer-by-layer deposition approach [30]. ITO-coated glass slides were employed as substrate (see Experimental). Due to the positive surface charge of the TiO_2 sol particles, ITO-coated glass slides immersed into the nanoparticle solution will readily adsorb a very thin nanoparticle coating. When this electrode is rinsed with water and methanol and then immersed into a Nafion® solution, binding of the anionic polymer and a restructuring of the surface occur. "Clustering" of TiO_2 nanoparticles into aggregates is observed. The electrode is then rinsed and re-immersed into the TiO_2 sol to continue the deposition process. An FEGSEM image of a two-layer TiO_2-Nafion® films is shown in Fig. 2a. It can be seen that the contact with the Nafion® anionomer causes nanoparticles to "cluster" into aggregates of about 40 nm diameter.

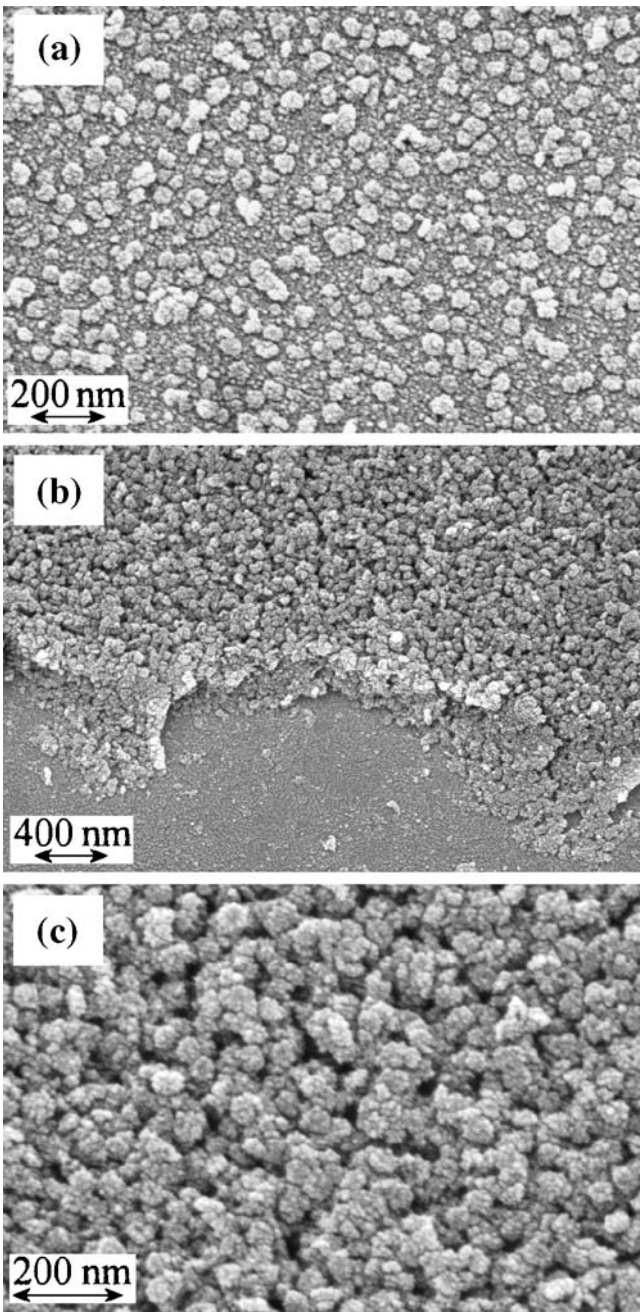

Fig. 2 FEGSEM images of **a** a 2-layer TiO_2-Nafion® film and **b**, **c** a 15-layer TiO_2-Nafion® film (scratched with a scalpel) on ITO substrate

When the deposition process is continued, more aggregates form, and they assemble into a porous structure. Figure 2b and c shows a 15-layer TiO_2-Nafion® film with pores of typically 10 to 30 nm diameter. These open pores create a hierarchical network, and this can be beneficial by allowing gas and fluids to penetrate into the nanocomposite film. The thickness of the porous film is controlled by the number of deposition cycles employed. Atomic force

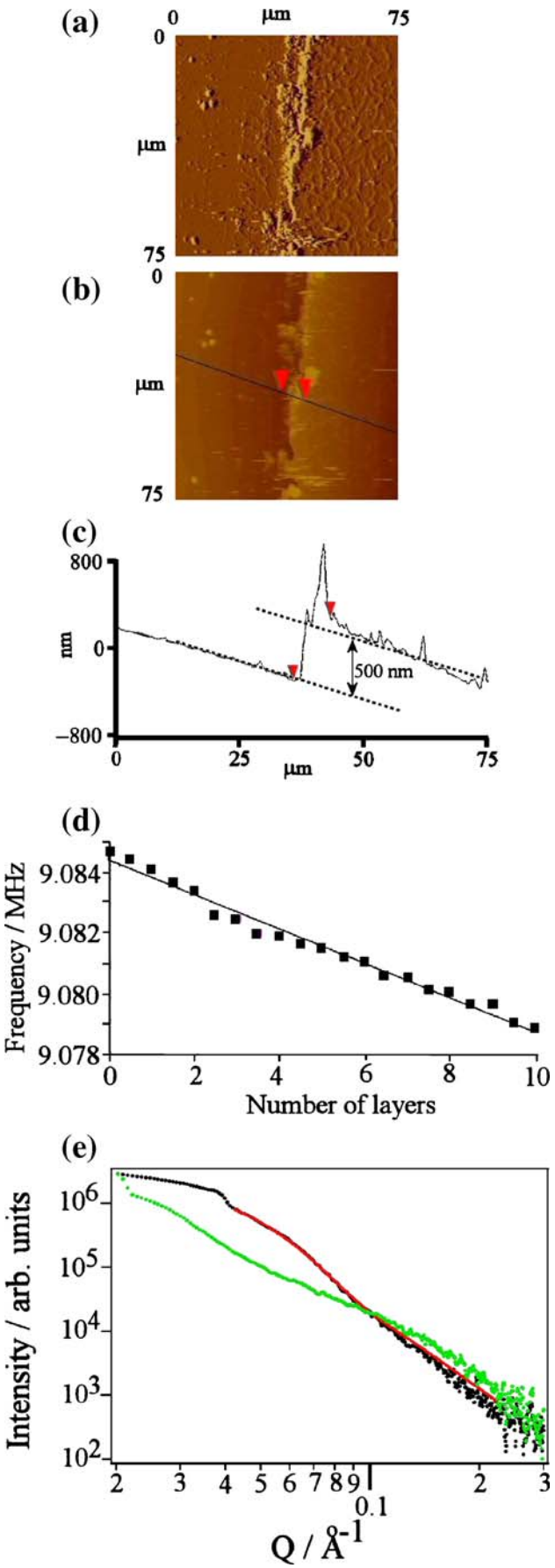

Fig. 3 AFM image data showing a 20-layer deposit of TiO_2-Nafion® ▶ on an ITO surface: **a**, **b** topography, **c** cross section. The surface has been scratched before to imaging. **d** Quartz crystal microbalance data obtained during deposition of consecutive TiO_2 and Nafion® layers onto an ITO-coated quartz resonator. **e** SAXS/WAXS data: experimental data for TiO_2 film only (*black*), for a TiO_2-Nafion® film (*green*), and for a theoretical fit for polydisperse TiO_2 spheres (mean radius, 38.81 Å; polydispersity, 0.295; *red line*)

microscopy images reveal the increase in thickness. An image of a 20-layer TiO_2-Nafion® film on an ITO substrate is shown in Fig. 3a and b. The film was scratched to reveal the cross section. The 20-layer film showed a height of about 500 nm (see Fig. 3c), which suggests a thickness of approximately 25 nm per deposition cycle which compares well with earlier studies employing other types of binder molecules [31].

Quartz crystal microbalance measurements at an ITO-coated quartz crystal oscillator were employed to quantify the weight change during the deposition of consecutive layers of the TiO_2-Nafion® nanocomposite. A plot of the frequency of the ITO resonator against the number of layers deposited is shown in Fig. 3d. This plot shows a linear build up of the TiO_2-Nafion® film with approximately 70 wt% contribution from TiO_2 and 30 wt% from Nafion®. These weight measurements were taken for dry films but may still contain small contribution from adsorbed water. The Sauerbrey equation allows the average weight to be calculated for TiO_2 particles deposited in one layer, 2,600 ng cm^{-2} (corresponding to 6×10^{12} TiO_2 particles using the density of the TiO_2 anatase particles 3.9 g cm^{-3}), and for Nafion® deposited in one layer, 1,000 ng cm^{-2}. These values are in good agreement with an average thickness per layer of 25 nm (vide supra).

Further characterization of the TiO_2-Nafion® nanocomposite films was obtained using the simultaneous SAXS/WAXS technique. Figure 3e shows the intensity of the scattered X-ray diffraction pattern for both TiO_2-Nafion® and pure (calcined) TiO_2 nanoparticle films. The experimental data can be fitted to a model (see red line) to determine the structure of the nanoparticle films.

The simulation model is that of isolated polydisperse spheres with a mean radius of 38.81 Å (assuming no interaction between each sphere) and is seen to give an excellent fit for the calcined TiO_2 film (treated at 500 °C in air for 30 min) between 0.04 and 0.1 $Å^{-1}$, indicating that there is no significant colloidal crystallinity. The small divergence between the fit and experimental data at greater values of Q may suggest possible interaction between spheres. A step in the intensity level is observed in the TiO_2-Nafion® and pure TiO_2 film at 0.04 $Å^{-1}$ and 0.08 $Å^{-1}$, respectively, which relates to the size of the particle or aggregate spheres. It is possible to establish that

the TiO_2-Nafion® aggregates are in average almost double the size of pure TiO_2 nanoparticles. However, a more complex composite structure is present, which is not easily modeled with conventional approaches. From FEGSEM image evidence (see Fig. 2), a raspberry-type packing or hierarchical clustering seems to occur. The step in intensity level at 0.02 $Å^{-1}$ and 0.04 $Å^{-1}$ in the TiO_2-Nafion® and pure TiO_2 films, respectively, can be attributed to an artifact generated after the subtraction of the background scattering pattern.

Electrochemical processes in TiO_2-Nafion® nanocomposite film electrodes

The voltammetric response observed for a clean ITO electrode immersed in aqueous 0.1 M KCl (used as an inert electrolyte) between 0.5 V vs SCE and −1.0 V vs SCE is featureless and consistent with a clean background (not shown). Figure 4 shows the voltammetric responses for a series of TiO_2-Nafion® films on ITO immersed in 0.1 M KCl. A reduction response commences at −0.7 V vs SCE, which is typical for a TiO_2 film, and is explained by the filling of the conduction band within the oxide [32]. Upon reversal of the scan direction, an oxidation peak is observed, which is consistent with electrons moving back from the oxide to the ITO substrate. The basic shape of the voltammograms can be explained by capacitive charging of the oxide and a resistance, which is mainly due to the ITO film [33]. The three different electrodes were 2, 10, and 20 layers of TiO_2-Nafion®. The increase in TiO_2 film thickness is demonstrated by the approximately proportional increase in the voltammetric response, which is associated with the reduction in Ti(IV) (vide infra).

To explore the reactivity of the TiO_2-Nafion® film in the presence of redox systems, three cationic redox systems with reversible one-electron characteristics have been chosen with reversible potentials close and more positive away from the TiO_2 conduction band edge.

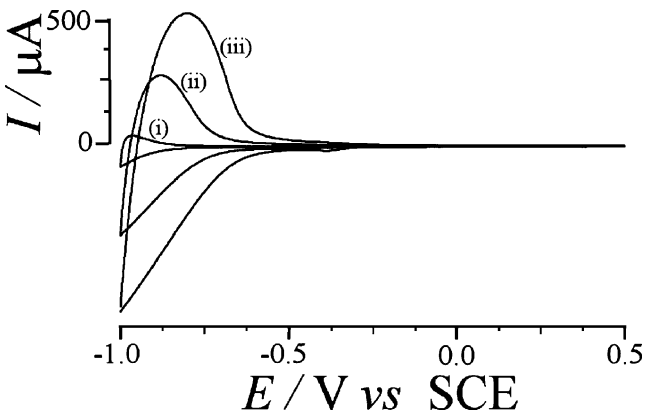

Fig. 4 Cyclic voltammograms (scan rate, 100 mV s^{-1}) for the reduction and oxidation of 6 nm TiO_2 nanoparticles bound by Nafion®, immobilized on ITO electrodes (area, 1 cm^2) immersed in 0.1 M KCl. *(i)* 2 layers TiO_2, *(ii)* 10 layers TiO_2,*(iii)* 20 layers TiO_2

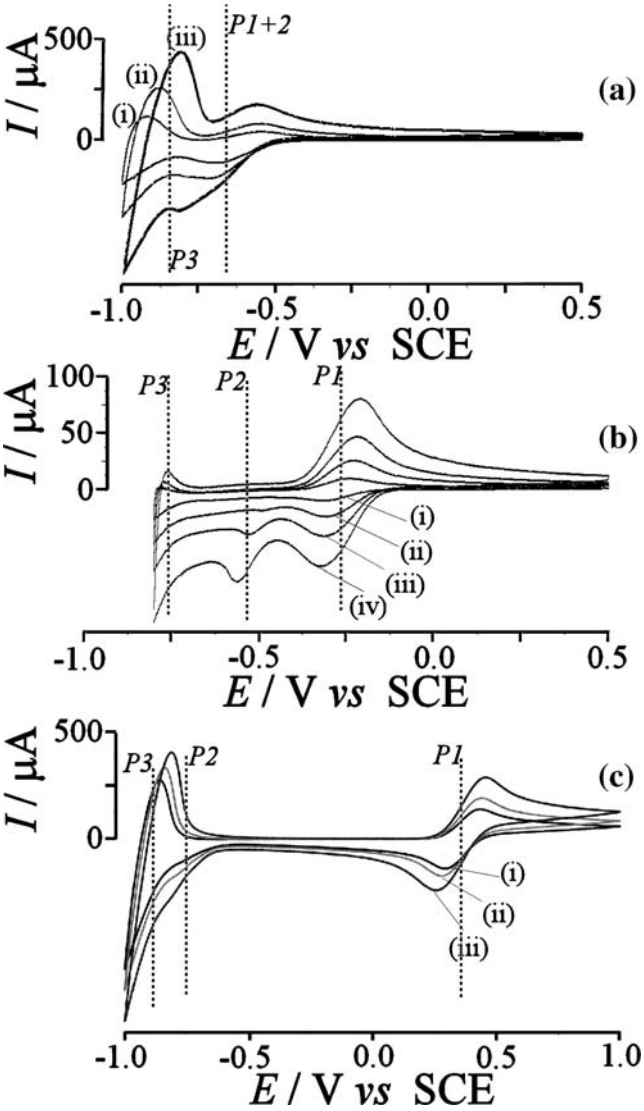

Fig. 5 **a** Cyclic voltammograms [scan rates *(i)* 20, *(ii)* 50, *(iii)* 100 mVs^{-1}] for the reduction and oxidation of 1,1′-diheptyl-4,4′-bipyridinium in a five-layer TiO_2-Nafion® film immobilized onto an ITO surface (area, 1 cm^2). The electrode was first immersed into a 1 mM solution of 1,1′-diheptyl-4,4′-bipyridinium dibromide in ethanol for 1 min, then rinsed with ethanol, and then the electrode was immersed in a 0.1 M KCl electrolyte. **b** Cyclic voltammograms [scan rates *(i)* 20, *(ii)* 50, *(iii)* 100, and *(iv)* 200 mVs^{-1}] for the reduction and oxidation of $Ru(NH_3)_6^{3+}$ in a 20-layer TiO_2-Nafion® film. The electrode was first immersed into 1 mM $Ru(NH_3)_6^{3+}$ in water, then rinsed with water, and then the electrode was immersed into a 0.1 M KCl electrolyte. **c** Cyclic voltammograms [scan rates *(i)* 20, *(ii)* 50, and *(iii)* 100 mVs^{-1}] for the reduction and oxidation of ferrocenylmethyl-trimethylammonium$^+$ in a 20-layer TiO_2-Nafion® film. The electrode was first immersed into 1 mM ferrocenylmethyl-trimethylammonium iodide in water, then rinsed with water, and then the electrode was immersed into a 0.1 M KCl electrolyte. *Dashed lines* indicate the approximate potential for redox processes

The 1,1′-diheptyl-4,4′-bipyridinium (or diheptylviologen) system exhibits a reversible redox process at −0.62 V vs SCE (see Fig. 5a) and a second reversible reduction step at more negative potentials (not shown) [34]. To obtain this response, a five-layer TiO_2-Nafion® film was immersed into a solution of 1,1′-diheptyl-4,4′-bipyridinium dibromide (1 mM in ethanol) for 1 min. The 1,1′-diheptyl-4,4′-bipyridinium was quickly immobilized into the Nafion® binder in the TiO_2-Nafion® film. The resulting electrode was then placed into aqueous 0.1 M KCl electrolyte, and a cyclic voltammogram was recorded.

In Fig. 5a, Process 1 (P1) denotes the reduction in 1,1′-diheptyl-4,4′-bipyridinium^{2+} to 1,1′-diheptyl-4,4′-bipyridinium^{+} by electrons directly from the ITO electrode surface (see Eq. 1). This particular mechanism operates solely at the ITO surface and requires molecular or charge diffusion within the Nafion® film. A second type of electron transfer is possible at more negative potentials, denoted as Process 2 (see Eq. 2). TiO_2 at sufficiently negative potentials is conducting electrons, and therefore direct electron transfer from TiO_2 becomes possible [35].

$$\text{Process 1}: [\text{Ox}]^{n+}(\text{Nafion}) + e^{-}(\text{ITO electrode}) \leftrightarrows [\text{Red}]^{(n-1)+}(\text{Nafion}) \quad (1)$$

$$\text{Process 2}: [\text{Ox}]^{n+}(\text{Nafion}) + e^{-}(TiO_2) \rightarrow [\text{Red}]^{(n-1)+}(\text{Nafion}) \quad (2)$$

$$\text{Process 3}: \text{Ti(IV)}(TiO_2) + e^{-}(\text{ITO elrctrode}) + H_2O \leftrightarrows \text{Ti(III)}(TiO_2) + H^{+}(TiO_2) + OH^{-} \quad (3)$$

A third process observed at potentials negative of −0.7 V vs SCE can be attributed to the conduction band filling of TiO_2 (see Fig. 4), which is associated with proton uptake (see Eq. 3). Next, a 20-layer TiO_2-Nafion® film is immersed into a solution of $Ru(NH_3)_6^{3+}$ (1 mM in water) for 1 min. The cationic $Ru(NH_3)_6^{3+}$ is immobilized into the Nafion® binder, and after rinsing with water, a reversible voltammetric response is observed at −0.25 V vs SCE (see Fig. 5b). This voltammetric signal occurs positive of the potential zone where TiO_2 is conducting and therefore can be attributed purely to Process 1 (Eq. 1). A new a separate irreversible reduction peak at −0.5 V vs SCE corresponds to Process 2, the $Ru(NH_3)_6^{3+}$ reduction via TiO_2 (Eq. 2).

Finally, a redox system with even more positive reversible potential was selected. Ferrocenylmethyl-trimethylammonium^{+} ($TMAFc^{+}$) is readily adsorbed into Nafion® and shows highly reversible electron transfer characteristics. A 20-layer TiO_2-Nafion® film was immersed into a solution of $TMAFc^{+}$ iodide (1 mM in water) for 1 min. The $TMAFc^{+}$ cation was immobilized into the Nafion® anionomer binder. The resulting electrode was then immersed into aqueous 0.1 M KCl electrolyte, and voltammograms were recorded (see Fig. 5c). A reversible response at 0.37 V vs SCE corresponds to Process 1 (Eq. 1), the one electron oxidation/reduction of $TMAFc^{+}$ by electrons directly from the ITO surface. A second reduction response is observed at −0.75 V vs SCE (see Process 2 of Eq. 2). The signal is irreversible and observed only immediately after scanning into the $TMAFc^{+}$ oxidation. It is interesting to note that the potential for Process 2 is dependent on the type of redox system, and this may reflect (1) the rate of electron transfer from TiO_2 to the molecular redox system and (2) the ability of the redox system to interact with the TiO_2 nanoparticle surface. More hydrophobic redox systems such as $TMAFc^{+}$ appear to interact less effectively with TiO_2, which may be responsible for the shift of Process 2 to more negative potentials.

Next, electron and charge transport within the mesoporous TiO_2-Nafion® film is investigated in more detail. By changing the film thickness and the potential scan rate, quantitative insights into the charge transfer and diffusion within the nanocomposite films can be obtained.

Charge diffusion in TiO_2-Nafion® nanocomposite film electrodes

By focusing on one particular redox system, ferrocenylmethyl-trimethylammonium^{+}, it is possible to further explore the effects of charge diffusion in the TiO_2-Nafion® composite material. Initially, a study of the adsorption characteristics of the ferrocenylmethyl-trimethylammonium cation ($TMAFc^{+}$) into the TiO_2-Nafion® films was undertaken. Figure 6 shows the experimental results indicating a reversible voltammetric response at a potential of 0.35 V vs SCE with increasing peak area as a function of $TMAFc^{+}$ immobilization concentration. Essentially Langmurian characteristics are observed, and for ferrocenylmethyl-trimethylammonium^{+}, a binding constant of 9,000 dm^3 mol^{-1} can be extracted.

The transport of charges in the porous TiO_2-Nafion® membrane is an interesting feature and must be connected to both (1) the mobility of an immobilized redox system such as $TMAFc^{+}$ and (2) intermolecular electron hopping. In the positive potential range TiO_2 is clearly electrically insulating, and charge transport along the pore walls within the mesoporous composite must be occurring. This was further confirmed by calcination of the TiO_2-Nafion® nanocomposite (this treatment at 500 °C in air fully removed all organic components and leaves a purely inorganic anatase film, see Fig. 3e) followed by re-adsorption of Nafion® from the dip coating solution (this

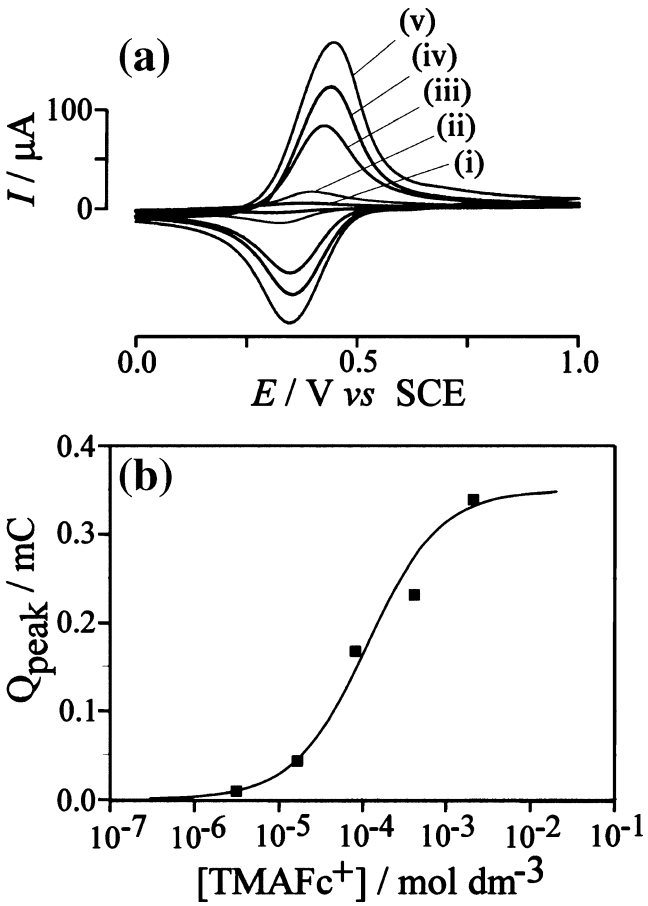

Fig. 6 **a** Cyclic voltammograms (scan rate, 0.1 V s^{-1}) for the oxidation and re-reduction of ferrocenylmethyl-trimethylammonium$^+$ immobilized into a five-layer TiO_2-Nafion® film at an ITO electrode surface (area, 1 cm^2) and immersed into aqueous 0.1 M $NaClO_4$. The ferrocenylmethyl-trimethylammonium$^+$ concentrations during the immobilizations step were *(i)* 3.2 μM, *(ii)* 16 μM, *(iii)* 80 μM, *(iv)* 0.4 mM, and *(v)* 2 mM in water. **b** Plot of the ferrocenylmethyl-trimethylammonium$^+$ concentration in the immobilization solution vs the charge under the voltammetric signal. The *line* shows a Langmuir dependence with a binding constant of K=9000 dm^3 mol^{-1}

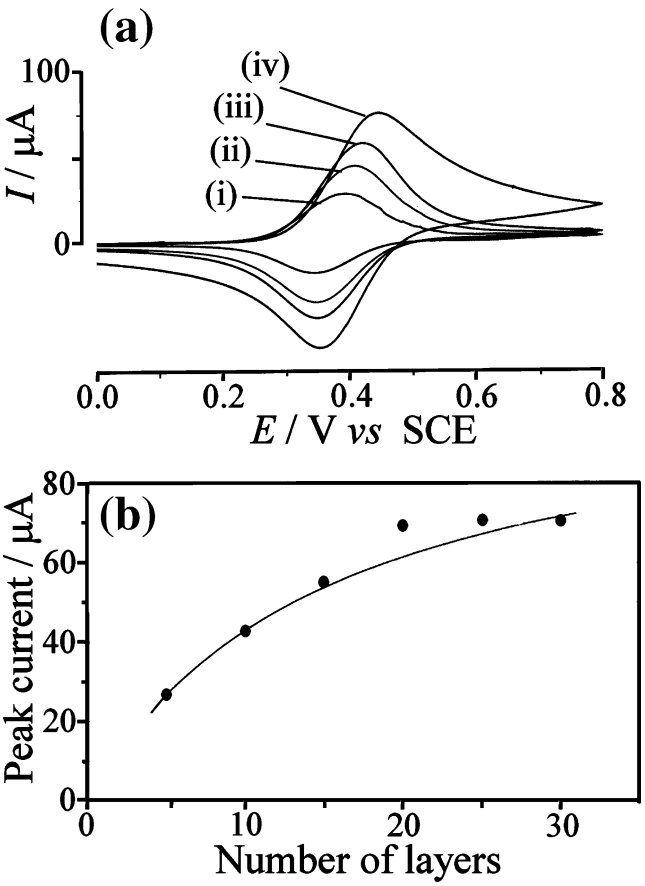

Fig. 7 **a** Cyclic voltammograms (scan rate, 0.02 V s^{-1}) for the oxidation and re-reduction of ferrocenylmethyl-trimethylammonium$^+$ immobilized into a *(i)* 5, *(ii)* 10, *(iii)* 15, and *(iv)* 30-layer TiO_2-Nafion® film at an ITO electrode surface (area, 1 cm^2) and immersed into aqueous 0.1 M $NaClO_4$. The ferrocenylmethyl-trimethylammonium$^+$ concentration during the immobilizations step was 2 mM in water. **b** Plot of the peak current vs the number of deposition layers. The *line* corresponds to a fit employing Eq. 6 with a concentration of c=0.1 M and an apparent diffusion coefficient of D=3.5×10^{-14} m^2 s^{-1}

process took approximately 24 h for a 20-layer film due to slow penetration of the anionomer back into the porous TiO_2). The resulting calcined film is believed to have much better TiO_2 particle–particle contacts but otherwise very similar dimensions. However, the voltammetric features did not change significantly (see below), and therefore, a contribution from the TiO_2 backbone to charge conductivity is highly unlikely.

To study the effect of the film thickness on the voltammetric features, a sequence of experiments was undertaken using a 2 mM ferrocenylmethyl-trimethylammonium$^+$ deposition solution and a 0.1 M $NaClO_4$ electrolyte solution (see Fig. 7). The increase in film thickness clearly resulted in an increase in the voltammetric peak current.

The relationship of the peak current with film thickness (see Fig. 7b) is not proportional, and at sufficiently thick films (about 1 μm), a stable peak current remains, completely independent of thickness. This transition in behaviour is consistent with a diffusion layer thickness in the mesoporous film. Approximate expressions can be written to describe this effect. The peak current for a complete electrolysis of the thin film at the electrode surface is given in Eq. 4 [36].

$$I_{p,\,\text{thin film}} = \frac{n^2F^2}{4RT}\nu Vc = \frac{n^2F^2}{4RT}\nu A\delta c \tag{4}$$

In this equation, the peak current is related to the number of transferred electrons per molecule diffusing to the electrode surface, n; the Faraday constant, F; the gas

constant, R; the absolute temperature, T; the scan rate, v; the electrode area, A; the film thickness, δ; and the concentration of redox active material, c. In contrast, for a thick film, a diffusion-controlled peak current (assuming a homogeneous material) is expected (see Eq. 5 [37]).

$$I_{p,\,\text{diffussion}} = 0.446nFAc\sqrt{\frac{nFvD}{RT}} \tag{5}$$

In this equation, the apparent diffusion coefficient is denoted by D. The transition of behaviour as a function of film thickness may be approximated by combining these two expressions in Eq. 6.

$$I_p = \frac{I_{p,\,\text{thin film}} \times I_{p,\,\text{diffusion}}}{I_{p,\,\text{diffussion}} + I_{p,\,\text{thin film}}} = \frac{n^2F^2vDAc\,\delta}{4RTD + 2.242\sqrt{RTDFnv}\,\delta} \tag{6}$$

Analysis of the thickness dependent voltammetric peak current data (see Fig. 7b and Eq. 6) suggests an approximate apparent diffusion coefficient of $D=3.5\times10^{-14}$ m^2 s^{-1} for ferrocenylmethyl-trimethylammonium$^+$. This value is very similar to the apparent diffusion coefficients reported for example for $Ru(bipy)_3^{3+/2+}$ in pure Nafion® [38, 39].

Next, the scan rate is systematically varied. In Fig. 8, voltammetric data for the oxidation of ferrocenylmethyl-trimethylammonium$^+$ immobilized in a five-layer TiO_2-Nafion® film are shown. A plot of the logarithm of the peak current vs the logarithm of the scan rate is expected to result in two linear regions: (1) a linear region with slope 1 due to thin film behaviour (see Eq. 4) and (2) a region with slope 0.5 due to diffusion within the film (see Eq. 5).

The plot in Fig. 8b clearly shows a transition between thin film and diffusion characteristics at a transition scan rate of $v_{\text{trans}}\approx0.05$ V s^{-1}. By combining Eqs. 4 and 5, an approximate expression for this transition can be obtained (Eq. 7).

$$D = \frac{nv_{trans}F}{RT}\left(\frac{\delta}{1.784}\right)^2 \tag{7}$$

For data in Fig. 8b, the apparent diffusion coefficient is calculated as $D\approx1\times10^{-14}$ m^2 s^{-1} in good agreement with the estimate obtained above. The thickness of the film δ introduces a considerable error into this calculation, and therefore, the methodology based on thickness variation is probably more accurate.

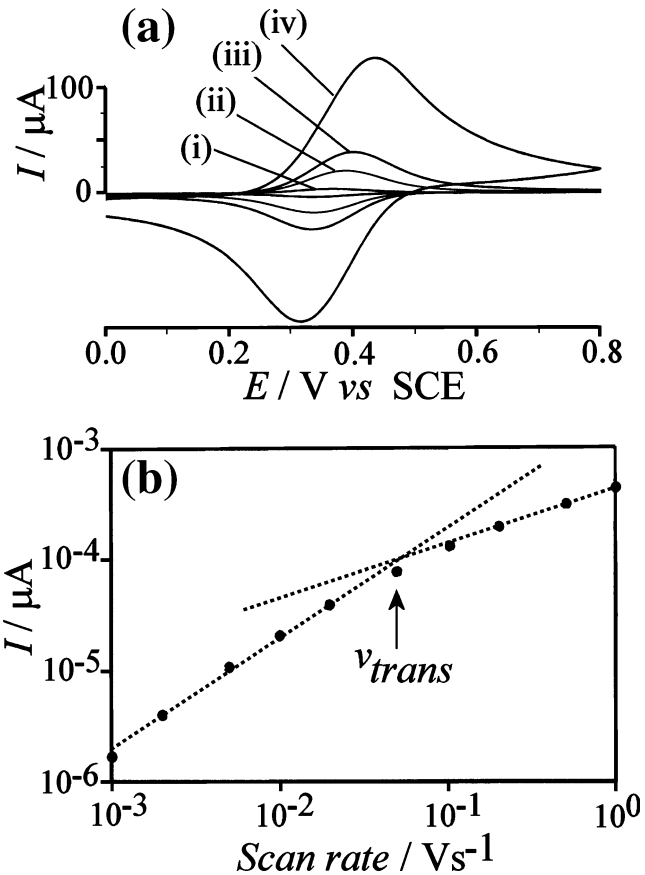

Fig. 8 **a** Cyclic voltammograms [scan rate *(i)* 0.002, *(ii)* 0.01, *(iii)* 0.02, *(iv)* 0.1 V s^{-1}] for the oxidation and re-reduction of ferrocenylmethyl-trimethylammonium$^+$ immobilized into a five-layer TiO_2-Nafion® film at an ITO electrode surface (area, 1 cm^2) and immersed into aqueous 0.1 $NaClO_4$. The ferrocenylmethyl-trimethylammonium$^+$ concentration during the immobilizations step was 2 mM in water. **b** Plot of the peak current for the oxidation peak vs scan rate

Conclusions

It has been shown that well-defined open-pore mesoporous structures are obtained by a layer-by-layer deposition of TiO_2 with Nafion® ionomer binder. TiO_2 particles of nominal 6 nm diameter tend to cluster into aggregates of about 20–40 nm size. The properties of the resulting films have been investigated, and redox reactions for three cationic redox systems have been studied. At potentials sufficiently positive of the conduction band edge, charge propagation/diffusion within the films is entirely due to electron hopping and molecular diffusion and very similar in magnitude when compared to processes in conventional Nafion® membrane systems. The open structure of these films allows fast diffusional access into the porous structure, and in future, this kind of membrane could be beneficial as a sensor film, or it could be employed as a host for proteins or enzymes.

Acknowledgement Tayca Corporation is acknowledged for providing a sample of TiO_2 colloidal solution. E.V.M. and S.J.S. are grateful for studentships awarded by the EPSRC and Royal Society of Chemistry. We acknowledge PANalytical for the generous provision of a SAXSess system used in the SAXS measurements included in this paper.

References

1. Varghese OK, Grimes CA (2003) J Nanosci Nanotech 3:277
2. Grätzel M (2005) MRS Bull 30:23
3. Schuth F (2005) Ann Rev Mater Res 35:209
4. Diebold U (2003) Surf Sci Rep 48:53
5. Bisquert J, Cahen D, Hodes G, Ruhle S, Zaban A (2004) J Phys Chem B 108:8106
6. Bavykin DV, Milsom EV, Marken F, Kim DH, Marsh DH, Riley DJ, Walsh FC, El-Abiary KH, Lapkin AA (2005) Electrochem Commun 7:1050
7. Bockmeyer M, Lobmann P (2006) Chem Mater 18:4478
8. Cameron PJ, Peter LM, Hore S (2005) J Phys Chem B 109:930
9. Ma TL, Kida T, Akiyama M, Inoue K, Tsunematsu SJ, Yao K, Noma H, Abe E (2003) Electrochem Commun 5:369
10. McKenzie KJ, King PM, Marken F, Gardner CE, Macpherson JV (2005) J Electroanal Chem 579:267
11. Stott SJ, Mortimer RJ, McKenzie KJ, Marken F (2005) Analyst 130:358
12. Decher G, Schlenoff (2003) Multilayer thin films. Wiley, Weinheim
13. McKenzie KJ, Marken F, Hyde M, Compton RG (2002) New J Chem 26:625
14. Murphy MA, Wilcox GD, Dahm RH, Marken F (2005) Ind J Chem A 44:924
15. Milsom EV, Novak J, Oyama M, Marken F (2007) Electrochem Commun 9:436
16. Correa-Duarte MA, Gierig M, Kotov NA, Liz-Marzan LM (1998) Langmuir 14:6430
17. Neivandt DJ, Gee M, Tripp CP, Hair ML (1997) Langmuir 13:2519
18. Serizawa T, Yamamoto K, Akashi M (1999) Langmuir 15:4682
19. Davis TA, Genders JD, Pletcher D (1997) Ion permeable membranes. The Electrochemical Consultancy, Romsey, UK
20. Shao ZG, Xu H, Li M, Hsing IM (2006) Solid State Ionics 177:779
21. Chalkova E, Fedkin MV, Wesolowski DJ, Lvov SN (2005) J Electrochem Soc 152:A1742
22. Park H, Choi W (2006) Langmuir 22:2906
23. Park H, Choi W (2005) J Phys Chem B 109:11667
24. Yuan S, Hu S (2004) Electrochim Acta 49:4287
25. Wang Y, Li C, Hu S (2006) J Solid State Electrochem 10:383
26. Bertoncello P, Notargiacomo A, Nicolini C (2005) Langmuir 21:172
27. Ward MD (1995) Physical electrochemistry. In: Rubinstein I (ed) Marcel Dekker, New York, p 297
28. Buttry DA, Anson FC (1982) J Am Chem Soc 104:4824
29. Mortimer RJ (1995) J Electroanal Chem 397:79
30. Farhat TR, Hammond PT (2006) Adv Func Mater 16:433
31. McKenzie KJ, Marken F (2003) Langmuir 19:4327
32. Marken F, Bhambra AS, Kim DH, Mortimer RJ, Stott SJ (2004) Electrochem Commun 6:1153
33. Fabregat-Santiago F, Mora-Sero I, Garcia-Belmonte G, Bisquert J (2003) J Phys Chem B 107:758
34. Mortimer RJ, Dillingham JL (1997) J Electroanal Chem 144:1549
35. Milson E, Perrott HR, Peter LM, Marken F (2005) Langmuir 21:9482
36. Bard AJ, Faulkner LR (2001) Electrochemical methods, 2nd edn. Wiley, New York, p 591
37. Scholz F (2002) Electroanalytical methods. Springer, Berlin Heidelberg New York, p 64
38. Majda M (1992) Molecular design of electrode surfaces In: Murray R (ed) Wiley, New York, p 200
39. Buttry DA, Anson FC (1983) J Am Chem Soc 105:685